02

Effect of crystal field local distortions on terahertz spectra of Pr^{3+} in langasite $Pr_3Ga_5SiO_{14}$

© A.M. Kuzmenko[1], V.Yu. Ivanov[1], A.Yu. Tikhanovskii[1], A.G. Pimenov[2], A.M. Shuvaev[2], A.A. Mukhin[1]

[1] Prokhorov Institute of General Physics, Russian Academy of Sciences, Moscow, Russia
[2] Institute of Solid State Physics, Vienna University of Technology, Vienna, Austria

E-mail: artem.kuzmenko.gpi@gmail.com

Received October 30, 2024
Revised November 25, 2024
Accepted February 28, 2025

The rare earth langasite $Pr_3Ga_5SiO_{14}$ (PGS) was studied using terahertz time-domain spectroscopy (TDS) at temperatures of $5-300$ K. In the frequency range of $5-40\,cm^{-1}$, a non-uniformly broadened absorption line was detected in the transmission and phase shift spectra of transmitted radiation, identified as a magnetic dipole transition between the levels of the ground quasi-doublet of the Pr^{3+} ion split by the crystal field. Strong non-uniform broadening is caused by random distortions of the local crystal field near rare earth ions. Consistent modeling of transmission spectra and static magnetic properties was carried out, which made it possible to establish the nature of the distribution of local distortions of the crystal field and determine the contribution of magnetic dipole transitions. Static magnetic properties are highly sensitive to the presence of local positions of Pr^{3+} ions with small splitting of the main quasi-doublet, while the main contribution to the terahertz resonance properties is made by ions with splitting near the maximum of the distribution and above.

Keywords: terahertz time-domain spectroscopy, rare-earth langasites, crystal field electron transitions.

DOI: 10.61011/EOS.2025.03.61154.4-25

Introduction

The langasite crystal $La_3Ga_5SiO_{14}$, first obtained in the 1980s [1], has a trigonal structure with space group $P321$ [2,3]. The replacement of the rare-earth ion La with strongly magnetic ions Pr [4–7], Nd [7–10] and Ho allowed the creation of new crystalline materials with magnetoelectric properties, which are attributable to the non-centrosymmetric chiral structure of langasite [5,11–14]. Due to their crystal structure, rare-earth langasites exhibit strong piezoelectric [15,16], laser and nonlinear optical properties [17–19], they show natural optical activity when radiation propagates along the trigonal axis [20–23]. However, the decrease of ionic radius in the series of rare earth elements allows growing crystals with complete La substitution only for Pr and Nd ions having the largest ionic radii close to La. For the remaining rare earths, single crystal growth was only possible for the substituted systems $(R_xLa_{1-x})_3Ga_5SiO_{14}$ (R = Gd, Tb, Dy, Ho).

The rare earth ion subsystem remains paramagnetic down to low temperatures both in fully substituted langasites Pr [5,24] and Nd [7,25–27] and in dilute systems $(Ho_xLa_{1-x})_3Ga_5SiO_{14}$ [12,28]. A number of interesting magnetic and magnetoelectric properties were found in these compositions [5,6,11,12]. The impact of the electronic structure of the Pr^{3+} ion on the magnetic and magnetoelectric properties of $Pr_3Ga_5SiO_{14}$ (PGS), the spectroscopic study of which is the subject of the present work, has been investigated in [5]. Pr^{3+} is a non-Kramers rare earth ion whose ground state in the langasite structure is a quasi-dublet — two singlet separated by a significant energy interval ($\sim 260\,cm^{-1}$) from the overlying levels (Fig. 1, *a*). This electronic structure leads to the Ising behavior of the magnetization of the main quasi-doublet of the ion, i.e., magnetization occurs only along one selected axis determined by the local crystal field. A similar ground state is realized in Ho^{3+} ions in $(Ho_xLa_{1-x})_3Ga_5SiO_{14}$ [12,28]. The splitting of the main quasidoublet Pr^{3+} $\sim 12\,cm^{-1}$ [5], whereas for Ho^{3+} $\sim 2\,cm^{-1}$ [28]. A broad distribution of the main quasidoublet parameters is observed for both ions due to distortions of the crystal field. These distortions can be both random, induced by elastic stresses and crystal defects (see, e.g., [29,30]) and related to the peculiarity of the langasite structure, namely, the presence of irregular crystallographic positions in which Si and Ga ions alternate (Fig. 1, *b*). Despite the similarities, there are significant differences in the distribution of ground state parameters due to crystal field distortions. A wide distribution of Ising directions of the magnetization axis of complex shape was observed in $(Ho_xLa_{1-x})_3Ga_5SiO_{14}$ [28]. In PGS no wide distribution of the directions of the Ising axes is found, but a distribution of the magnitude of the quasi-dublet splitting in the crystal field is realized, the width of which is comparable to the position of the maximum of the distribution [5].

Terahertz spectroscopic study of PGS allows direct observation of the effects associated with crystal field distortions reflected in the broadening of the absorption line associated with electronic transitions between states of the main quasi-doublet Pr^{3+}.

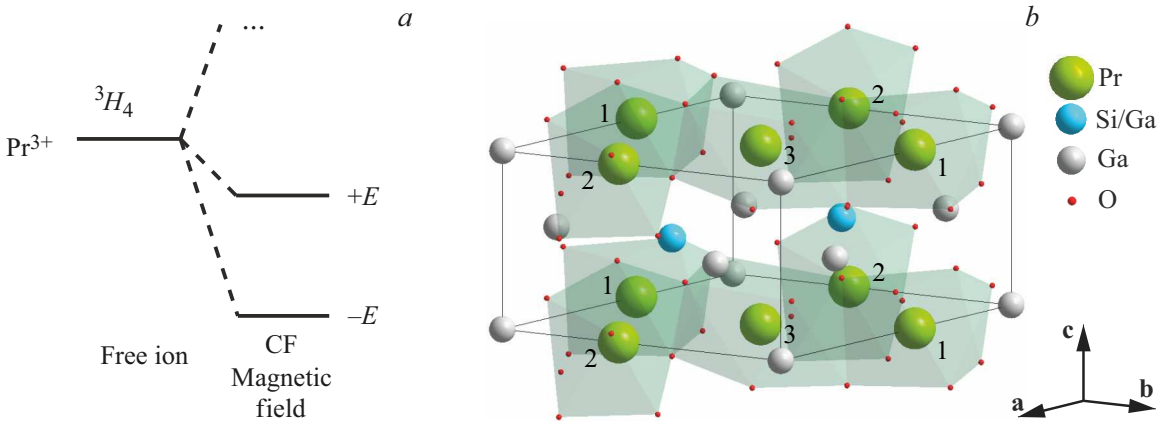

Figure 1. Diagram of the splitting of the main quasi-doublet in the crystal and external magnetic fields (*a*). Crystal structure of PGS (*b*).

Experiment

Large single crystals $Pr_3Ga_5SiO_{14}$ were grown by a zone melting method with radiation heating [4]. Plane-parallel samples were prepared from cylindrical crystals with diameters ~ 5 mm, with slices of thickness $\sim 1-2$ mm oriented perpendicular to the crystallographic axes. The transmission and phase shift spectra of the past emission of PGS were studied by terahertz time domain spectroscopy (TDS) methods in the frequency range of $5-100\,cm^{-1}$ and temperature range of $5-300$ K (Fig. 2–4). The samples of *a*- and *c*-sections for radiation polarizations $\mathbf{h} \parallel \mathbf{c}\,\mathbf{e} \parallel \mathbf{b}^*$ (Fig. 2), $\mathbf{h} \parallel \mathbf{b}^*\,\mathbf{e} \parallel \mathbf{a}$ (Fig. 3) and $\mathbf{h} \parallel \mathbf{b}^*\,\mathbf{e} \parallel \mathbf{c}$ (Fig. 4), the orientations of the magnetic **h** and electric **e** fields relative to the crystallographic axes (the axis $\mathbf{b}^*$ is perpendicular to the axes **a** and **c**) are indicated. The observed oscillations in transmittance and phase are attributable to the interference in a plane-parallel sample.

A strong increase of absorption at high frequencies associated with phonon modes is a common feature of the spectra. The positions and intensities of phonon modes in PGS for polarizations of the alternating electric field **e** along and perpendicular to the trigonal axis **c** of the crystal are consistent with the estimates made in Ref. [9] based on a study of infrared reflectance spectra. The increased contribution of this phonon mode leads to a strong low-temperature increase of the dielectric constant along the axis **c** at low frequencies [9]. The low frequency and high intensity of the phonon in the $\mathbf{e} \parallel \mathbf{c}$ polarization make it difficult to observe using TDS. However, studying a sample with a small thickness of $d = 0.07$ mm allowed the edge of this phonon mode to be detected in the spectra (Fig. 4). A similar intense low-frequency phonon mode [9] was observed in langasite with complete substitution of La by Nd, whose ionic radius is close to Pr. The line position, intensity, and width of the low-lying phonon modes change with temperature change.

A broad absorption line was detected in the spectra against the phonon dispersion background in the more transparent polarizations of radiation $\mathbf{h} \parallel \mathbf{c}\,\mathbf{e} \parallel \mathbf{b}^*$ (Fig. 2) and $\mathbf{h} \parallel \mathbf{b}^*\,\mathbf{e} \parallel \mathbf{a}$ (Fig. 3). This line was identified as a magnetic-dipole transition between the states of the ground quasi-doublet of Pr ions in the crystal field (Fig. 1, *a*). The line intensity sharply drops as the temperature increases, which is consistent with the temperature dependence of the magnetization [5].

Analysis and discussion of experimental results

The transmission spectra were analyzed using the plane-wave approximation, with the **e** and **h** components of linearly polarized radiation aligned along the crystallographic axes, thereby maintaining their linear polarization during propagation. The spectra were modeled using Fresnel formulas for a plane-parallel layer, taking into account the dispersion of the complex dielectric (ε^*) and magnetic (μ^*) permeabilities near the resonant lines as Lorentz oscillators:

$$\varepsilon^*(\nu) = \varepsilon'(\nu) + i\varepsilon''(\nu) = \varepsilon_\infty + \sum_k \Delta\varepsilon_k \frac{\nu_k^2}{\nu_k^2 - \nu^2 - i\nu_k\gamma_k}, \quad (1)$$

$$\mu^*(\nu) = \mu'(\nu) + i\mu''(\nu) = 1 + \sum_k \Delta\mu_k \frac{\nu_k^2}{\nu_k^2 - \nu^2 - i\nu_k\gamma_k}, \quad (2)$$

where ν_k — resonant frequencies, $\Delta\mu_k$ and $\Delta\varepsilon_k$ — contributions to magnetic and dielectric permeabilities (determining line intensities), γ_k — the line width of the *k*-th oscillator, ε_∞ — the high-frequency dielectric permittivity.

The dielectric oscillators $\Delta\varepsilon_k$ in (1) describe phonon modes whose frequencies lie above the investigated range, but the strong dispersion of the dielectric permittivity near these intense excitations affects the transmission and phase shift of the emission near the observed magnetic Pr lines. The dispersion of the dielectric permittivity (1) is described in each of the studied geometries $\mathbf{e} \parallel \mathbf{a}, \mathbf{b}^*, \mathbf{c}$ (Fig. 2–4) by a single oscillator corresponding to the underlying phonon; the contribution of the other phonons is accounted for in ε_∞.

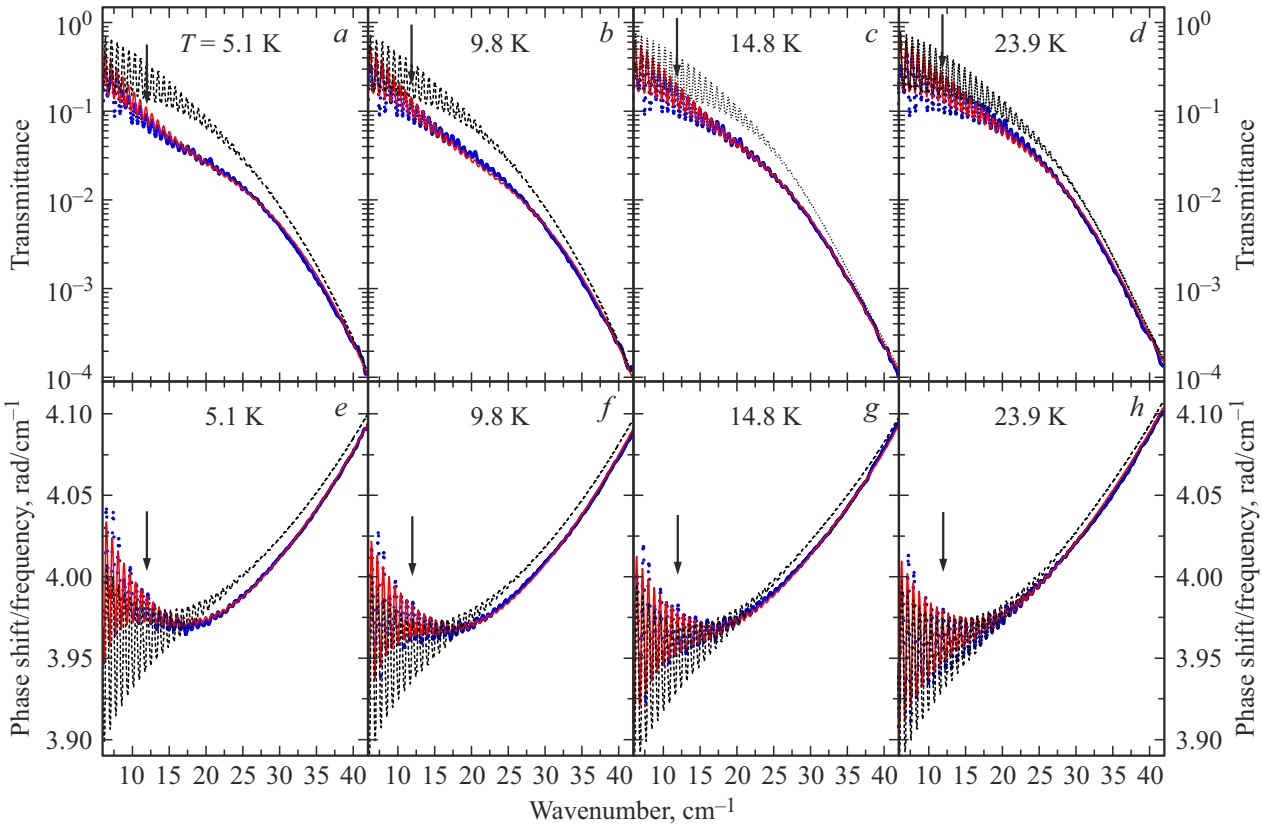

Figure 2. Low-temperature terahertz transmission spectra (a, b, c, d) and past emission phase shift (e, f, g, h) of PGS in $\mathbf{h} \parallel \mathbf{c}\,\mathbf{e} \parallel \mathbf{b}^*$ polarization. Experiment data are shown by dots, results of simulation with and without considering the ground state contribution of Pr^{3+} ions are shown by solid and dashed lines, respectively. The arrows indicate the frequency corresponding to the maximum position $\rho_{Gxx}(\Delta)$.

The parameters of phonon modes were estimated: in polarizations $\mathbf{e} \parallel \mathbf{a}, \mathbf{b}^*$ at temperature $T = 5\,\mathrm{K}$ $\Delta\varepsilon^{a,b^*} = 12 \pm 2$, $\nu^{a,b^*} = 110 \pm 2\,\mathrm{cm}^{-1}$, $\gamma^{a,b^*} = 20 \pm 5\,\mathrm{cm}^{-1}$; in polarization $\mathbf{e} \parallel \mathbf{c}$ at $T = 21\,\mathrm{K}$ $\Delta\varepsilon^{c} = 75 \pm 8$, $\nu^{c} = 28 \pm 5\,\mathrm{cm}^{-1}$, $\gamma^{c} = 15 \pm 5\,\mathrm{cm}^{-1}$. These estimates are consistent with Ref. [9].

The strongly broadened absorption line at frequencies $\sim 20\,\mathrm{cm}^{-1}$ (Fig. 2, 3) is associated with the paramagnetic subsystem of Pr^{3+} ions. The non-uniform broadening of the observed mode is attributable to distortions of the crystal field leading to the distribution of the parameters of the main quasi-doublet, in particular its splitting in the crystal field, which in the absence of an external magnetic field determines the frequency of the corresponding transition. The occurrence of local distortions of the crystal field can be associated to varying degrees with the distribution of random elastic stresses, the presence of lattice defects, as well as the presence in the structure of langasite irregular crystallographic positions with alternation of Si and Ga ions, the distribution of which can form a superstructure [2]. The analysis of magnetic and magnetoelectric properties performed in Ref. [28] for the substituted composition $(Ho_xLa_{1-x})_3Ga_5SiO_{14}$, showed the similarity of distortion parameter distributions of the crystal field for samples of different quality grown by the zone melting method and the Czochralski method. This behavior indicates that the distribution of distortions in rare earth langasites is not random, depending on the quality of a particular sample, but depends significantly on the irregular Si/Ga positions near the rare earth, i. e., it is a property of the crystal structure. However, the specific mechanism of distortion requires further study.

The studies of magnetization and magnetic field-induced electric polarization performed in Ref. [5] showed that the quasi-doublet of the ground state of the noncrameric ion Pr^{3+} in langasite is separated by a significant energy interval $(\sim 180\,\mathrm{cm}^{-1})$ from the excited states [5]. This electronic configuration leads to the Ising character of the magnetization of the main quasi-doublet Pr^{3+}, i.e., to a strong anisotropy of g-factor, in which the magnetization in an external field occurs along one selected direction determined by the crystal field.

Next, let us perform a concerted analysis of the high-frequency and static magnetic properties of PGS at low temperatures, where they are determined mainly by the transitions within the main quasi-doublet and the Van Vleck contribution to the static magnetic susceptibility due to the admixture of excited states. It should be noted that the line shape could not be satisfactorily described by a single Lorentz oscillator in (2), which confirms the non-uniform

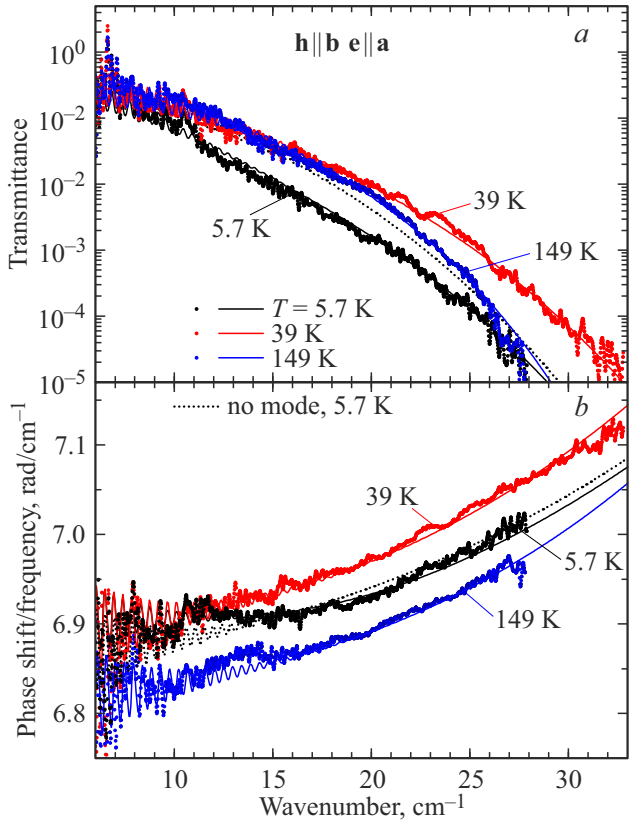

Figure 3. Terahertz transmission spectra (a) and phase shift of the past emission (b) of PGS in the polarization $\mathbf{h} \parallel \mathbf{b}^* \mathbf{e} \parallel \mathbf{a}$ at different temperatures. Dots — experiment, solid lines — simulation result, dashed line (no mode) — simulation result of the spectrum for 5.7 K without taking into account the ground state contribution of Pr^{3+} ions.

nature of the broadening because of distortions of the crystal field.

The energy levels of the quasi-dublet of the i-th ion are equal to $\pm E_i = \sqrt{\Delta_i^2 + (\mathbf{m}_i \mathbf{H})^2}$, and the total splitting of the quasi-doublet is $2E_i$ (Fig. 1, a), where Δ_i splitting in the crystal field; $\mathbf{m}_i \mathbf{H} = m_0 \mathbf{n}_i \mathbf{H} = -i\mu_B g_J \langle A|\hat{\mathbf{J}}_i \mathbf{H}|B\rangle$ ($|A\rangle$ and $|B\rangle$ — wave functions of the quasi-doublet) [5,12], $\mathbf{n}_i$ — unit vector directed along the Ising axis; $\mathbf{H}$ — external magnetic field.

The terahertz magnetic susceptibility of PGS in the frequency region of magnetodipole electronic transitions between states of the main quasi-doublet Pr^{3+} at $H = 0$, when $E_i = \Delta_i$, can be represented ([31,32]) as

$$\chi_R^{jk}(\nu, T) = N \frac{m_i^j m_i^k}{\Delta_i} \tanh \frac{\Delta_i}{k_B T} \frac{\Delta_i^2}{\nu_i^2 - \nu^2}, \qquad (3)$$

where m_i^j is the j-component of the magnetic moment of the transition, $\nu_i = 2\Delta_i/(2\pi\hbar)$ is the resonance frequency, $\hbar$ is the Planck constant, $N = 3/V_{cell}$ is the number of Pr ions in 1 cm^3, V_{cell} is the lattice cell volume of the crystal, k_B is the Boltzmann constant.

The trigonal symmetry of the crystal implies three local directions of the Ising axes for different crystallographic positions of Pr^{3+}. In this case, the local second-order symmetry axis C_2 for a particular crystallographic position coincides with one of the three second-order symmetry axes of the crystal. It should be noted here that, depending on the wave functions of the quasi-dublet, the directions of the Ising axes are possible either along or perpendicular to the local axis **a**. The anisotropy of the magnetization [5] indicates the position of the Ising axes in the $\mathbf{b}^*\mathbf{c}$-plane at an angle of 45.5° to the axis **c**. The presence of trigonal symmetry of the crystal implies that the orientation of the Ising axis in one of three types of crystallographic positions, such as $\mathbf{m}_1$, is related to the other two positions by rotation matrices $C_3^{\pm}$ by ±120° around the axis **c** of the crystal: $\mathbf{m}_{2,3} = C_3^{\pm}\mathbf{m}_1$ (see position numbers in Fig. 1, b).

Random distortions of the local crystal field were described in Ref. [5], when modeling static magnetic properties using a Rayleigh distribution for the crystal-field splitting Δ:

$$\rho_R(\Delta) = \frac{\Delta}{\sigma^2} e^{-\Delta^2/2\sigma^2}. \qquad (4)$$

However, in our case, it was not possible to obtain a satisfactory description of the resonant absorption by such a distribution Δ. The parameters obtained to describe the

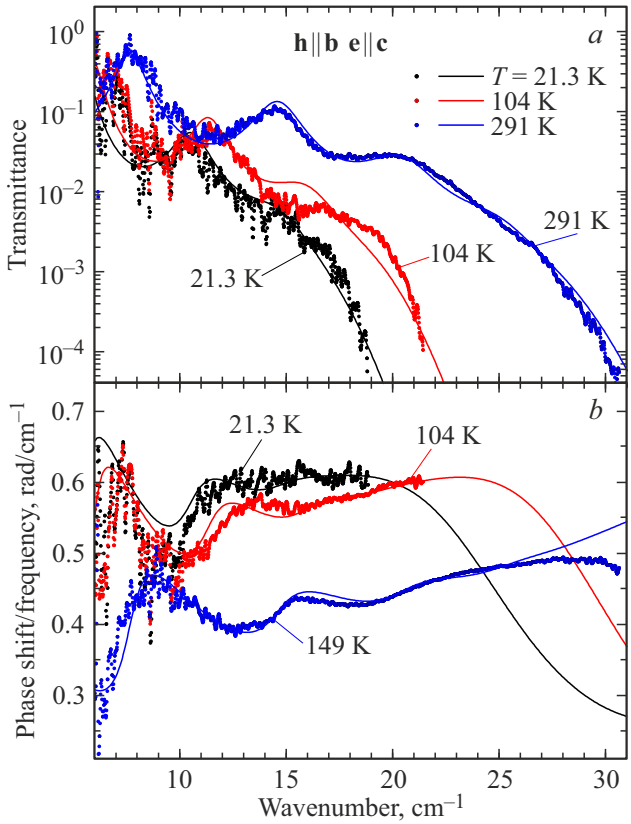

Figure 4. Terahertz transmission spectra (a) and phase shift of the transmitted emission (b) of PGS in $\mathbf{h} \parallel \mathbf{b}^* \mathbf{e} \parallel \mathbf{c}$ polarization at different temperatures. Dots — experiment, lines — simulation result.

magnetization give too high position of the maximum of the distribution $\rho(\Delta)$, which is not consistent with the results of terahertz measurements. Reducing the position of the maximum leads to too strong low-temperature magnetization growth, which is due to an increase in the number of ions with small splitting values Δ. Thus, magnetization measurements and terahertz spectra prove sensitive to different regions of the function $\rho(\Delta)$: the dominant contribution to low-temperature magnetization comes from states with small crystal-field splittings, whereas in terahertz spectra, the most pronounced absorption and phase shift arise from states near the maximum $\Delta_{\max}$ of the function $\rho(\Delta)$ and higher-energy states Δ, which correspond to higher frequencies. A different distribution function was used with these considerations in mind. The Rayleigh distribution (4) $\rho R(\Delta) \sim \Delta G(\Delta)$, where $G(\Delta)$ is the Gaussian distribution, does not grow smoothly enough near $\Delta = 0$. The spectra near the resonant modes and static magnetization are simultaneously described in this paper using the distribution $\rho_{Gxx}(\Delta) \sim \Delta^2 G(\Delta)$:

$$\rho_{Gxx}(\Delta) = \eta_{Gxx}(\xi, \sigma)\Delta^2 \exp\left(\frac{1}{2}\left(\frac{\Delta - \xi}{\sigma}\right)^2\right), \qquad (5)$$

where $\eta_{Gxx}(\xi, \sigma)$ is a multiplier that ensures the normalization condition: $\int_0^{+\infty} \rho(x)dx = 1$; ξ, σ are parameters of the distribution that determine its maximum position $\Delta_{\max}$ and width, $\xi = \Delta_{\max} - 2\sigma^2/\Delta_{\max}$. For example, the Maxwell distribution for particle velocities is a special case of such a distribution. Fig. 5 shows an example of comparing the shape of the distributions $\rho_{Gxx}(\Delta)$ and $\rho_R(\Delta)$. Both of these functions reflect the observed character of the resonance line, which has a broad absorption maximum whose position is comparable to its width, but the difference near $\Delta = 0$ affects the static and resonance properties most significantly.

Let us model the experimental transmission spectra and phase shift measured at zero external permanent field ($H = 0$) in the $\mathbf{h} \parallel \mathbf{a}, \mathbf{b}^*$ and $\mathbf{c}$ polarizations by deriving an expression for the complex magnetic permeability $\mu^j = 1 + 4\pi\chi_R^{jj}$ along the corresponding axis based on (3) taking into account the distribution $\rho_{Gxx}(\Delta)$ (5) and the presence of three non-equivalent crystallographic positions q (Fig. 1, *b*):

$$\mu^{a,b^*,c}(\nu, T) = 1 + 4\pi \frac{N}{3} \sum_{q=1}^{3} \int_{\Delta=0}^{\infty} (m_q^{a,b^*,c})^2 \times \frac{1}{\Delta} \tanh \frac{\Delta}{k_B T} R(\nu)\rho_{Gxx}(\Delta)d\Delta, \qquad (6)$$

where $R_i(\nu) = \nu_i^2/(\nu_i^2 - \nu^2)$ is the resonance multiplier.

Fig. 2, 3 show examples of the description of spectra taking into account the dispersion of dielectric (1) and magnetic (6) permeabilities in polarizations $\mathbf{h} \parallel \mathbf{c}\,\mathbf{e} \parallel \mathbf{b}^*$ and $\mathbf{h} \parallel \mathbf{b}^*\,\mathbf{e} \parallel \mathbf{a}$ for different temperatures. The magnetic transition moment modulus m_0 and the parameters of distribution $\rho_{Gxx}(\Delta)$: $\Delta_{\max}$ and σ were the varying parameters for

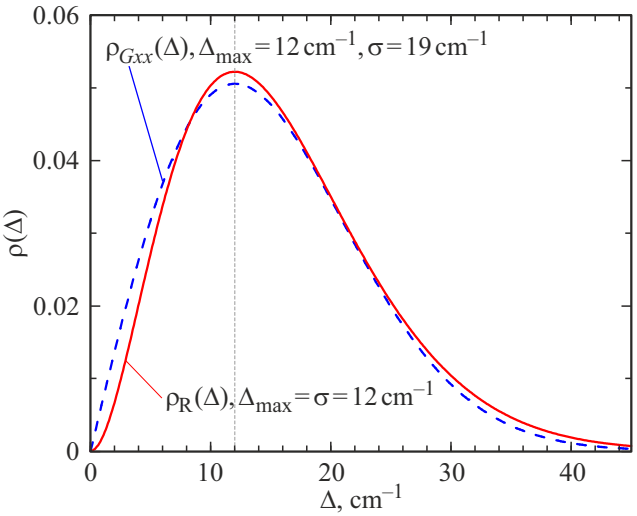

Figure 5. Densities of distribution $\rho_{Gxx}(\Delta)$ with parameters determined from simulations of terahertz spectra and static magnetization (dashed line), and the Rayleigh distribution $\rho_R(\Delta)$ with parameters providing a similar curve shape (solid line).

modeling the contributions to the magnetic permeabilities μ_c^* and $\mu_{b^*}^*$. The directions of the Ising axes are taken from Ref. [5]. The expression for the static magnetization is obtained as described in Ref. [5,12,28]:

$$\mathbf{M} = \frac{N}{3} \sum_q \int \mathbf{m}_q(\mathbf{H}\mathbf{m}_q) \frac{1}{E_q(\Delta)} \times \tanh \frac{E_q(\Delta)}{k_B T} \rho_{Gxx}(\Delta)d\Delta + \chi_{VV}^{a,b^*,c}\mathbf{H}, \qquad (7)$$

where $\chi_{VV}^{a,b^*,c}$ is the Van Vleck magnetic susceptibility. The experimental dependences of magnetization from Ref. [5] on the external magnetic field (Fig. 6, *a, b*) and temperature (Fig. 6, *c*) are described using the expression (7).

The given theoretical dependences both for terahertz spectra (Fig. 2, 3) and for magnetization (Fig. 6) are constructed with the same parameters determining the magnetic contribution of the main quasi-doublet ion Pr^{3+}: $m_0 = (2.3 \pm 0.1)\,\mu_B$ — the magnetic moment modulus at each of the positions q; $\Delta_{\max} = 12 \pm 1\,\text{cm}^{-1}$ and $\sigma = 19 \pm 5\,\text{cm}^{-1}$; $\chi_{VV}^{a,b^*} = (2.3 \pm 0.3) \cdot 10^{-5}\,\text{cm}^3/\text{g}$, $\chi_{VV}^{c} = (2.0 \pm 0.3) \cdot 10^{-5}\,\text{cm}^3/\text{g}$.

Conclusion

The electronic transitions between the lower levels of the main multiplet of Pr^{3+} ion in the langasite crystal $Pr_3Ga_5SiO_{14}$ have been directly observed using the method of terahertz spectroscopy in the frequency range of $2-35\,\text{cm}^{-1}$. The analysis allowed identifying and quantitatively describing the features of strong non-uniform broadening of the resonance line associated with the

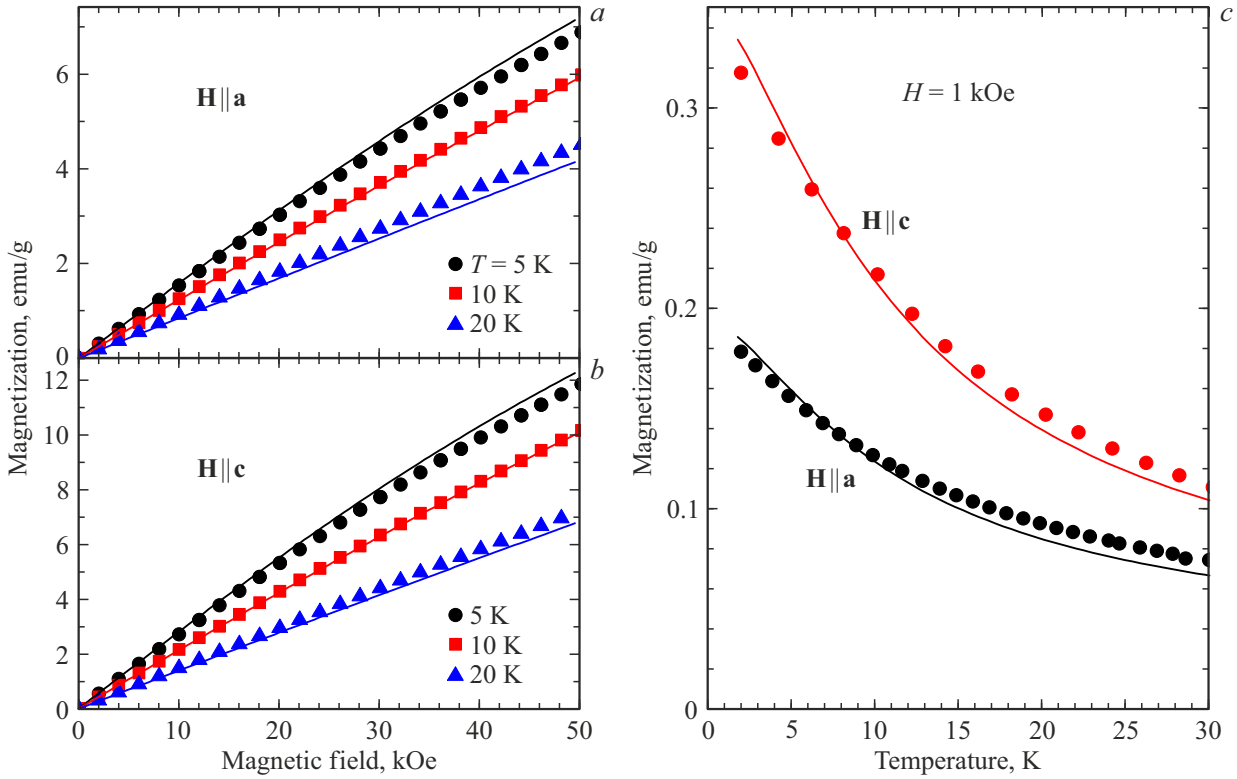

Figure 6. Magnetization curves (a, b) and temperature dependences of magnetization at $H = 1$ kOe (c) of PGS for different orientations of **H**. Dots — experiment [5], lines — simulation result.

distribution of local distortions of the crystal field near the rare-earth ion, leading to changes of the splitting of the main quasi-doublet Pr^{3+}.

It should be noted that the distribution of splittings in the crystal field can have a much more complex structure. In addition to a wide distribution of random distortions, the crystal probably realizes the presence of several groups of distributed positions associated with different symmetry of the rare-earth ion environment near different combinations of alternating Si/Ga positions (Fig. 1, *b*). It is not possible to resolve the positions of individual maxima in case of large widths of random distortion distributions, which is clearly demonstrated by the broad homogeneous modes in the transmission spectra. The clarification of the shape and nature of the distortion distribution requires further precision measurements of the transmission and phase spectra are needed at frequencies below 10 cm^{-1}, at which TDS techniques have not yet yielded reliable results.

Funding

This study was financially supported by the Russian Science Foundation (project №22-42-05004).

Conflict of interest

The authors declare that they have no conflict of interest.

References

[1] B.V. Mill, Y.V. Pisarevsky. In: *Proceedings of the 2000 IEEE/EIA International Frequency Control Symposium and Exhibition* (IEEE, Kansas City, 2000), p. 133. DOI: 10.1109/FREQ.2000.887343

[2] Y. Yoneda, H. Takeda, T. Shiosaki, J. Mizuki. Jpn. J. Appl. Phys., **46**, 7163 (2007). DOI: 10.1143/JJAP.46.7163

[3] B.A. Maksimov, V.N. Molchanov, B.V. Mill, E.L. Belokoneva, M.K. Rabadanov, A.A. Pugacheva, Y.V. Pisarevskii, V.I. Simonov. Crystallogr. Reports, **50**, 751 (2005). DOI: 10.1134/1.2049391

[4] A.P. Dudka, A.M. Balbashov. Kristallografiya **65**, 223 (2020) (in Russian). DOI: 10.31857/S0023476120020058

[5] A. Tikhanovskii, V.Y. Ivanov, A. Kuzmenko, E. Constable, A. Pimenov, A. Mukhin. Phys. Rev. B, **110** 014409 (2024). DOI: 10.1103/PhysRevB.110.014409

[6] A. Zorko, F. Bert, P. Mendels, K. Marty, P. Bordet. Phys. Rev. Lett., **104**, 057202 (2010). DOI: 10.1103/PhysRevLett.104.057202

[7] P. Bordet, I. Gelard, K. Marty, A. Ibanez, J. Robert, V. Simonet, B. Canals, R. Ballou, P. Lejay. J. Phys. Condens. Matter., **18**, 5147 (2006). DOI: 10.1088/0953-8984/18/22/014

[8] V. Simonet, R. Ballou, J. Robert, B. Canals, F. Hippert, P. Bordet, P. Lejay, P. Fouquet, J. Ollivier, D. Braithwaite. Phys. Rev. Lett., **100**, 237204 (2008). DOI: 10.1103/PhysRevLett.100.237204

[9] L. Bergen, L. Weymann, J. Wettstein, A.M. Kuzmenko, A.A. Mukhin, B.V. Mill, A. Pimenov, E. Constable. Phys. Rev. B, **104**, 024106 (2021). DOI: 10.1103/PhysRevB.104.024106
[10] N.N. Zhang, J.Y. Wang, X.R. Pan, M.J. Song, C.D.S. Clenilton, G.D.G. Ilde. Jiegou Huaxue, **35**, 1673 (2016). DOI: 10.14102/j.cnki.0254-5861.2011-1200
[11] A.A. Mukhin, V.Y. Ivanov, B.V. Mill. In: *Book of Abstracts, Moscow International Symposium on Magnetism* (Faculty of Physics Lomonosov Moscow State University, M., 2017), p. 663.
[12] L. Weymann, L. Bergen, T. Kain, A. Pimenov, A. Shuvaev, E. Constable, D. Szaller, B.V. Mill, A.M. Kuzmenko, V.Y. Ivanov, N.V. Kostyuchenko, A.I. Popov, A.K. Zvezdin, A. Pimenov, A.A. Mukhin, M. Mostovoy. Npj Quantum Mater., **5**, 61 (2020). DOI: 10.1038/s41535-020-00263-9
[13] A.P. Oreshko, E.N. Ovchinnikova, A. Rogalev, F. Wilhelm, B.V. Mill, V.E. Dmitrienko. J. Synchrotron Radiat., **25**, 222 (2018). DOI: 10.1107/S1600577517015387
[14] A.P. Oreshko, B.V. Mill, E.N. Ovchinnikova, A. Rogalev, F. Wilhelm, V.E. Dmitrienko. Crystallogr. Rep. **63**, 158 (2018). DOI: 10.1134/S1063774518020189
[15] K. Shimamura, H. Takeda, T. Kohno, T. Fukuda. J. Cryst. Growth, **163**, 388 (1996). DOI: 10.1016/0022-0248(95)01002-5
[16] N. Araki, H. Ohsato, K. Kakimoto, T. Kuribayashi, Y. Kudoh, H. Morikoshi. J. Eur. Ceram. Soc., **27**, 4099 (2007). DOI: 10.1016/j.jeurceramsoc.2007.02.177
[17] A.A. Kaminskii, S.E. Sarkisov, B.V. Mill, G.G. Khodzhabagyan. Inorg. Mater., **18**, 1189 (1982).
[18] A.A. Kaminskii, B.V. Mill, I.M. Silvestrova, G.G. Khodzhabagyan. Izv. Acad. Sci. USSR, Phys. Ser., **47**, 1903 (1983).
[19] H. Lan, F. Liang, Z. Lin, H. Yu, H. Zhang, J. Wang. Int. J. Opt., **2017**, 1 (2017). DOI: 10.1155/2017/2980274
[20] A.F. Konstantinova, T.G. Golovina, A.P. Dudka, N.L. Sizova. Crystallogr. Reports, **67**, 398 (2022). DOI: 10.1134/S1063774522030105
[21] V.I. Burkov, O.A. Lysenko, B.V. Mill. Crystallogr. Reports, **55**, 983 (2010). DOI: 10.1134/S1063774510060131
[22] Y. Shopa, N. Ftomyn, I. Sokoliuk. Ukr. J. Phys. Opt., **15**, 155 (2014). DOI: 10.3116/16091833/15/3/155/2014
[23] T.G. Golovina, A.F. Konstantinova, A.P. Dudka, A.V. Butashin, B.A. Umanskii, N.S. Kozlova, V.M. Kasimova, E.V. Zabelina. Crystallogr. Reports, **68**, 732 (2023). DOI: 10.1134/S106377452360045X
[24] L.L. Lumata, T. Besara, P.L. Kuhns, A.P. Reyes, H.D. Zhou, C.R. Wiebe, L. Balicas, Y.J. Jo, J.S. Brooks, Y. Takano, M.J. Case, Y. Qiu, J.R.D. Copley, J.S. Gardner, K.Y. Choi, N.S. Dalal, M.J.R. Hoch. Phys. Rev. B, **81**, 224416 (2010). DOI: 10.1103/PhysRevB.81.224416
[25] H.D. Zhou, B.W. Vogt, J.A. Janik, Y.-J. Jo, L. Balicas, Y. Qiu, J.R.D. Copley, J.S. Gardner, C.R. Wiebe. Phys. Rev. Lett., **99**, 236401 (2007). DOI: 10.1103/PhysRevLett.99.236401
[26] A. Zorko, F. Bert, P. Mendels, P. Bordet, P. Lejay, J. Robert. Phys. Rev. Lett., **100**, 147201 (2008). DOI: 10.1103/PhysRevLett.100.147201
[27] Q.J. Li, Z.Y. Zhao, H.D. Zhou, W.P. Ke, X.M. Wang, C. Fan, X.G. Liu, L.M. Chen, X. Zhao, X.F. Sun. Phys. Rev. B, **85**, 174438 (2012). DOI: 10.1103/PhysRevB.85.174438
[28] A.Y. Tikhanovskii, V.Y. Ivanov, A.M. Kuzmenko, A. Stunault, O. Fabelo, E. Ressouche, V. Simonet, R. Ballou, I.A. Kibalin, A. Pimenov, A.A. Mukhin, E. Constable. Phys. Rev. B, **109** 214433 (2024). DOI: 10.1103/PhysRevB.109.214433
[29] B.Z. Malkin, D.S. Pytalev, M.N. Popova, E.I. Baibekov, M.L. Falin, K.I. Gerasimov, N.M. Khaidukov. Phys. Rev. B, **86**, 134110 (2012). DOI: 10.1103/PhysRevB.86.134110
[30] A.M. Kuzmenko, A.A. Mukhin, V.Y. Ivanov, G.A. Komandin, A. Shuvaev, A. Pimenov, V. Dziom, L.N. Bezmaternykh, I.A. Gudim. Phys. Rev. B, **94**, 174419 (2016). DOI: 10.1103/PhysRevB.94.174419
[31] A.A. Mukhin, A.S. Prokhorov. Trudy IOFAN, **25**, 162 (1990). (in Russian).
[32] P. Fulde. *Handbook on the physics and chemistry of rare earths: Alloys and intermetallics*, ed. by K.A. Gschneidner, J. Eyring, L. Eyring (North-Holland, Amsterdam, 1979), vol. 2, ch. 17. DOI: 10.1016/S0168-1273(79)02008-0

Translated by A.Akhtyamov